AMERICAN SOCIETY FOR MICROBIOLOGY | Infection and Immunity®

MICROBIAL IMMUNITY AND VACCINES

# Development of a Monoclonal Antibody to a Vibriophage as a Proxy for *Vibrio cholerae* Detection

Md Abu Sayeed,[a] Taylor Paisie,[b] Meer Taifur Alam,[c] Afsar Ali,[a,c] Andrew Camilli,[d] Jens Wrammert,[e] Ashraful Islam Khan,[f] Firdausi Qadri,[f] Marco Salemi,[b] J. Glenn Morris,[c] Eric J. Nelson[a,c,g]

[a]Department of Environmental and Global Health, University of Florida, Gainesville, Florida, USA
[b]Department of Pathology, University of Florida, Gainesville, Florida, USA
[c]Emerging Pathogens Institute, University of Florida, Gainesville, Florida, USA
[d]Department of Molecular Biology and Microbiology, Tufts University School of Medicine, Boston, Massachusetts, USA
[e]Department of Microbiology and Immunology, Emory University School of Medicine, Atlanta, Georgia, USA
[f]International Centre for Diarrhoeal Disease Research, Bangladesh (icddr, b), Dhaka, Bangladesh
[g]Department of Pediatrics, University of Florida, Gainesville, Florida, USA

**ABSTRACT** Cholera is an acute watery, diarrheal disease that causes high rates of morbidity and mortality without treatment. Early detection of the etiologic agent of toxigenic *Vibrio cholerae* is important to mobilize treatment and mitigate outbreaks. Monoclonal antibody (mAb) based rapid diagnostic tests (RDTs) enable early detection in settings without laboratory capacity. However, the odds of an RDT testing positive are reduced by nearly 90% when the common virulent bacteriophage ICP1 is present. We hypothesize that adding a mAb for the common, and specific, virulent bacteriophage ICP1 as a proxy for *V. cholerae* to an RDT will increase diagnostic sensitivity when virulent ICP1 phage is present. In this study, we used an *in-silico* approach to identify immunogenic ICP1 protein targets that were conserved across disparate time periods and locations. Specificity of targets to cholera patients with known ICP1 was determined, and specific targets were used to produce mAbs in a murine model. Candidate mAbs to the head protein demonstrated specificity to ICP1 by Enzyme linked immunosorbent assay (ELISA) and an ICP1 phage neutralization assay. The limit of detection of the final mAb candidate for ICP1 phage particles spiked into cholera stool matrix was $8 \times 10^5$ PFU by Western blotting analysis. This mAb will be incorporated into a RDT prototype for evaluation in a future diagnostic study to test the guiding hypothesis behind this study.

**KEYWORDS** bacteriophage, vibriophage, phage, ICP1, *Vibrio cholerae*, cholera, Bangladesh, rapid diagnostic tests (RDT), diarrhea

Cholera continues as one of the most important public health problems since the 19th century, especially in resource-limited settings. Cholera can result in severe dehydration and death if untreated (1). The ongoing seventh cholera pandemic started in Indonesia in 1961 (2). Cholera remains endemic in regions of south-east Asia and Africa where there is a lack of safe drinking water, hygiene, and improved sanitation (2, 3). It is estimated that 1.3 to 4.0 million cholera cases occur globally annually with 21,000 to 143,000 deaths (1, 4, 5). The frequency of cholera outbreaks is likely to rise due to globalization, rapid urbanization, and climate change (6, 7). The causative agent for cholera is toxigenic *Vibrio cholerae*, a Gram-negative facultative anaerobe. *V. cholerae* can be classified into two biotypes, classical and El Tor, more than 200 serogroups (O1-O200), and two serotypes for O1, Ogawa and Inaba. Out of all serotypes, *V. cholerae* El Tor, O1, Ogawa and Inaba are the main etiologic agents for cholera outbreaks (8, 9).

Cholera outbreaks in endemic settings follow a seasonal pattern. During outbreaks, cholera patients shed hyper-infectious *V. cholerae* as well as virulent bacteriophages

**Editor** Andreas J. Bäumler, University of California, Davis



Address correspondence to Md Abu Sayeed, msayeed@ufl.edu.

The authors declare no conflict of interest.

**Received** 18 April 2022
**Returned for modification** 23 May 2022
**Accepted** 29 June 2022
**Published** 18 July 2022

(phages) (10). The proportion of cholera positive stool samples carrying virulent phage likely increases over the course of an outbreak and can reach 100% (11). It is hypothesized that the predation of virulent phages influences the seasonal pattern of cholera epidemics in cholera endemic regions (10–13). Three primary virulent phages (ICP1, ICP2, ICP3) have been found in the stool of cholera patients in Bangladesh (14, 15). ICP1, a member of the *Myoviridae* bacteriophage family, is the most prevalent phage excreted in cholera patient's stool during the episode of an epidemic (14, 16, 17). ICP1 phage is specific to *V. cholerae* O1 and has been in other geographical locations, including India and Africa (South Sudan and Democratic Republic of Congo [DRC]) (16–19).

According to the World Health Organization, it is estimated that more than 90% of the annual cholera cases are not reported (20). The underestimation of cholera incidence acts as a barrier for planning and implementation of acute and long-term mitigation. Lack of resources for diagnostics and appropriate surveillance systems in cholera prone areas is one of the major reasons for underreporting (2, 5, 21) and delayed public health responses. A rapid and accurate point of care diagnostic test can expedite cholera surveillance, response, and, ultimately, reduce mortality and morbidity (22–24).

The gold standards for cholera diagnosis are microbial culture and PCR for the detection of *V. cholerae* from stool samples. However, the sensitivity of culture method alone is approximately 70% and requires at least 2 to 3 days in a well-equipped microbiology laboratory with trained personnel (16, 25–28). PCR for the detection of pathogens is an alternative to the culture because of its higher sensitivity of approximately 85% (8, 29). PCR is more rapid than conventional culture, but this technique requires expensive reagents and molecular equipment as well as trained laboratory staff.

Rapid diagnostic tests (RDTs) can be used by minimally trained staff at the bed side without requiring a cold-chain or advanced equipment. More than 20 cholera RDTs have been developed (20). Most are based on immunochromatographic immunoassays, targeting *V. cholerae* O1 lipopolysaccharide antigen (30–32). Laboratory and field evaluation of RDTs showed a wide range of sensitivity and specificity of around 32% to 100%, and 60% to 100%, respectively (4, 16, 24). RDT performance metrics are variable, which largely limits their scope of use to cholera detection and surveillance. Our group has shown previously that virulent phage ICP1 and antibiotic exposure negatively impact RDT performance. The odds of cholera RDT test positivity decreases by up to 90% when ICP1 phage is present (10, 16). To address this limitation, we hypothesized that adding an antibody for ICP1 to the RDT will be associated with an increase in sensitivity without compromising specificity when ICP1 phage is present in cholera stool (Fig. 1). In this study, we used *in-silico*, *in vitro,* and *in vivo* techniques to develop a mAb that demonstrates specificity for the ICP1 phage, with the goal to incorporate the phage mAb into the RDT and evaluate the novel RDT in a future diagnostic study.

## RESULTS

**Selection and characterization of ICP1 protein targets for monoclonal antibody production.** Eleven conserved ICP1 bacteriophage target open reading frames (ORFs) were identified and evaluated *in-silico* for immunogenic epitopes using VaxiJen and The Immune Epitope Database (IEDB) tools. The target ORFs were predicted to be highly antigenic with antigenicity scores of 0.54 to 1.03 (threshold of predicted antigen 0.4) by Vaxigen (Table S2). The targets were cross verified by IEDB to confirm antigenic epitopes (Table S2).

For further study, we selected the two putative structural proteins: a putative baseplate protein (ORF75) and a putative major head protein (ORF122). Analysis was performed on these targets to assess conservation by time and location. Conservation was found at both the nucleic acid and amino acids levels (Fig. 2A and B, and Fig. S2A and B). However, ORF75 demonstrated higher rates of genetic diversity over time (Fig. 2C and Fig. S2C) compared to ORF122 (Fig. 2D and Fig. S2D). The target ORF75 from the type-strain ICP1 from Bangladesh (ICP1_2011_A) showed 92% (709/774) similarity at the nucleotide level and 97% (249/257) similarity at the amino acid level, compared to an ICP1 isolate from Africa (DRC; ICP1_DRC_106) by a Clustal Omega sequence alignment. The target ORF122 from the type-strain ICP1 from Bangladesh (ICP1_2011_A) showed 99.8%

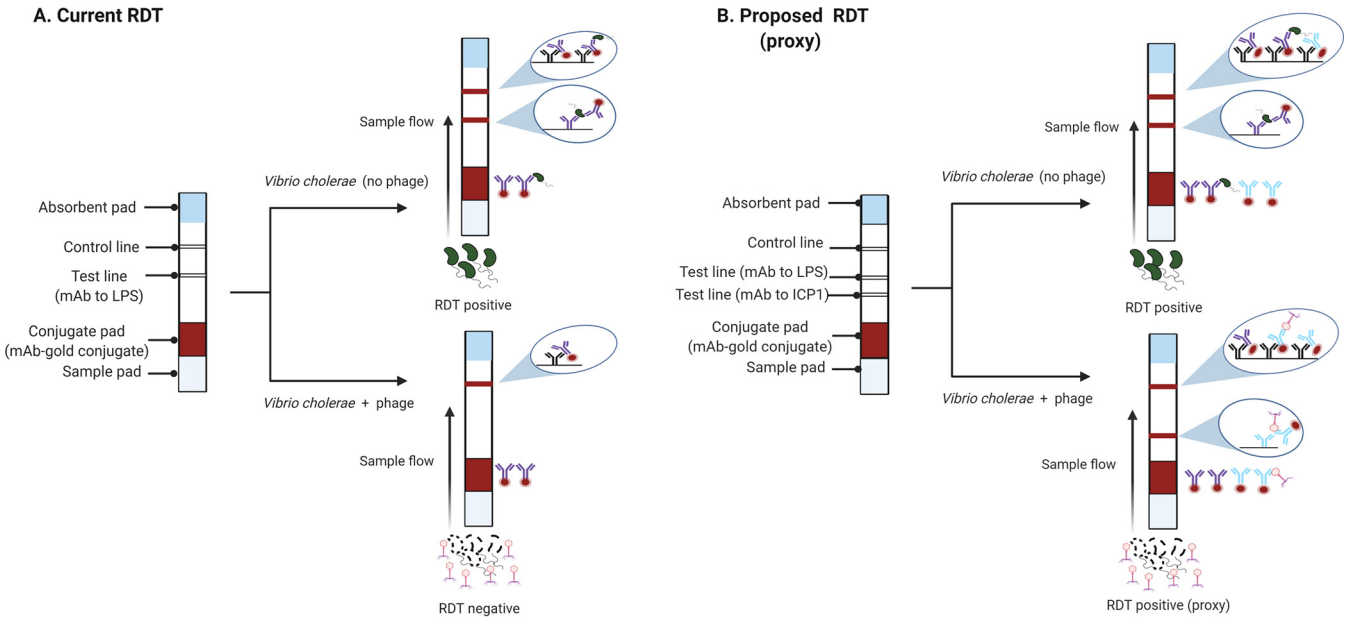


**FIG 1** A model showing how an RDT for *V. cholerae* may fail when virulent phage (e.g., ICP1) are present in a stool sample (A) and how this limitation can be addressed by incorporating a mAb to phage as a proxy for *V. cholerae* when phage are present (B).

(1018/1020) similarity at the nucleotide level and 99.7% (338/339) similarity at the amino acid level compared to an ICP1 isolate from Africa (DRC; ICP1_DRC_106) (Fig. S1).

For Fig. 2A and B displaying the amino acid multi-sequence alignments (MSA), we detected a small amount of non-synonymous (dN) mutations. We observed more dN mutations in ORF75 than in ORF122. The temporal signal in Fig. 2C and D highlights the conservation of ORF75 and ORF122, where the temporal signal can infer whether or not accumulating mutations are observed over time and a data set with an accumulation of mutations overtime would be displayed with a positive slope in the temporal signal plots. A neutral slope and negative slope were observed for ORF75 (Fig. 2D) and ORF122 (Fig. 2D), respectively. Similar findings were observed at the nucleotide level (Fig. S2).

The ORF75 and ORF122 targets were screened (present/absent) by PCR in 12 phage and *V. cholerae* negative (10 from Bangladesh and 2 from Africa [South Sudan]), 2 ICP1 phage negative and *V. cholerae* positive (one from Bangladesh and one from Africa [South Sudan]), and 2 both ICP1 phage and *V. cholerae* positive stool samples (one from Bangladesh and one from Africa [South Sudan]). The ORFs were not detected in ICP1 negative stools (cholera or non-cholera). The ICP1 positive stools from both Bangladesh and Africa (South Sudan) were positive for ORF75 and ORF122 (Table S3).

**Evaluation of monoclonal antibody (mAb) candidates by ELISA.** Enzyme linked immunosorbent assay (ELISA) was used. Culture supernatants of ORF75 hybridoma clones showed minimal to no reactivity to ICP1 bacteriophage in contrast to positive reactivity with purified ORF75 protein; cross-reactivity to ICP2, and ICP3 was not detected (Fig. 3A). In contrast, 19 out of 20 culture supernatants of ORF122 hybridoma clones were reactive to ICP1 and purified ORF122; cross-reactivity to ICP2 and ICP3 was not detected. The relative responses to ICP1 were significantly higher in comparison to ICP2, ICP3, formalin-killed *V. cholerae* whole-cell (VCWC) and Bovine serum albumin (BSA); but was comparable with purified ORF122 protein (Fig. 3B). Given the failure of the ORF75 candidate mAbs to detect native ICP1, these candidates were eliminated from further analysis. Three ORF122 hybridoma clones including clone 5 (ICP1ORF122_mAbCL5), clone 6 (ICP1ORF122_mAbCL6), and clone 14 (ICP1ORF122_mAbCL14) were selected for further analysis based on high reactivity to ICP1.

**Evaluation of head protein mAb candidates by Western blot analysis.** The three candidate ORF122 hybridoma clone supernatants were analyzed by Western blotting.

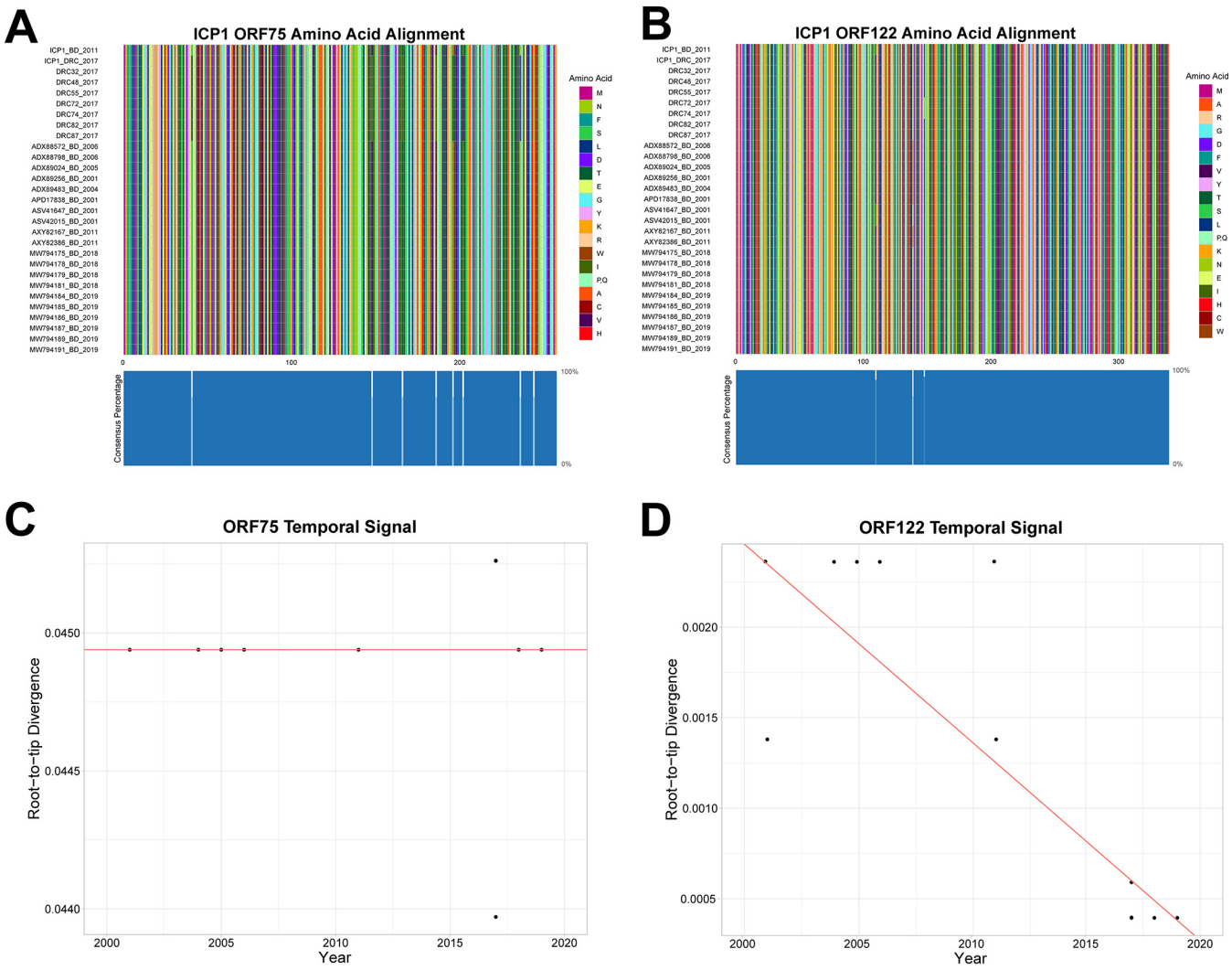


**FIG 2** Multi-sequence alignment of ICP1 phage baseplate ORF75 (A) and capsular head ORF122 (B) amino acid sequences. Sequences from both Bangladesh (BD) and Democratic Republic of Congo (DRC). Blue boxes at the bottom of 'A' and 'B' represent the percentage of the isolates that have the same amino acid for that particular site. Temporal and divergence analysis of baseplate ORF75 (C) and capsular head ORF122 (D) nucleotide sequences from ICP1 phage isolated from Bangladesh.

All three clones detected ICP1 as well as purified ORF122 recombinant protein. Cross-reactivity was not observed among the negative controls (ICP2, ICP3, VCWC, BSA, and phosphate-buffered saline [PBS]) (Fig. 4A). All three candidate mAb clone supernatants detected ICP1 isolates from the disparate locations for Bangladesh and Africa (Goma DRC) (Fig. 4B).

**Evaluation of head protein mAb candidates by phage neutralization assay analysis.** We characterized the three ICP1 reactive ORF122 clone supernatants using a phage neutralization assay. All three mAb supernatant clones showed statistically significant neutralization of ICP1 (Fig. 5); ICP1ORF122_mAb CL5, CL6 and CL14 were able to neutralize 31%, 42%, and 39% ICP1 bacteriophage, respectively, in comparison to control (only PBS). The reduction in plaque counts by phage neutralization for all the clones were statistically significant ($P < 0.001$) (Fig. 5A).

**Limit of mAb detection of ICP1 bacteriophage in cholera stool matrix by Western blot analysis.** We determined the limit of detection of ICP1 phage for the two final candidate clone supernatants (ICP1ORF122_mAb CL5 and CL6). We spiked ICP1 bacteriophage into ICP1 negative and *V. cholerae* negative stool samples in 3-fold dilution series. We found that both CL5 and CL6 culture supernatants (1:500) were able to detect down to $8 \times 10^5$ PFU of ICP1 bacteriophage by Western blot (Fig. 6).

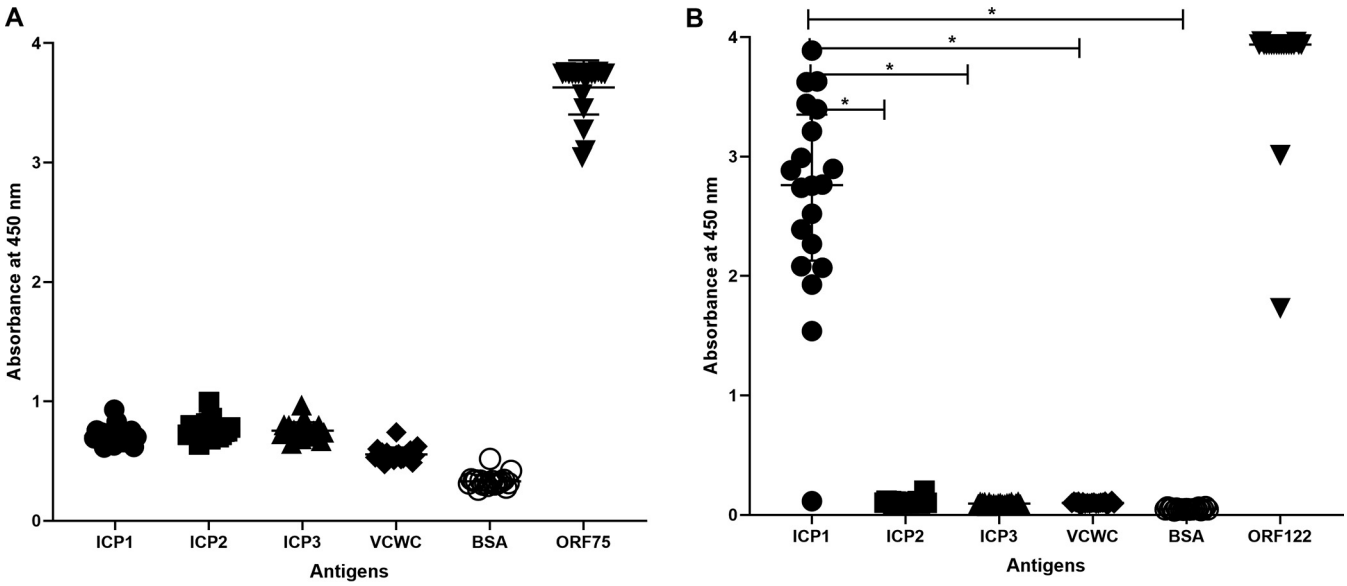


**FIG 3** Immunoreactivity by ELISA of ORF75 mAbs ($n$ = 20) (A) and ORF122 mAbs ($n$ = 20) (B) to phage particles (ICP1, ICP2, ICP3), formalin-killed *V. cholerae* whole-cell (VCWC), bovine serum albumin (BSA) and ORF75 and ORF122 recombinant protein. Statistically significant differences ($P < 0.05$) in the mean immune response from all clones are denoted with an asterisk. Symbols represent the average of three technical replicates for one mAb from one experiment; data are representative of two independent experiments. The $y$ axis is set to the maximal absorbance in the assay.

## DISCUSSION

In this study, we aimed to develop a mAb against the common virulent vibriophage ICP1 as a critical step toward addressing limitations with current cholera RDTs. Our guiding hypothesis is that adding a mAb for ICP1 to the existing RDT as a proxy for *V. cholerae* will increase sensitivity when ICP1 degrades the primary *V. cholerae* target. We used an *in-silico* approach to identify immunogenic protein targets that were conserved and specific to cholera patients. Candidate proteins were expressed for mAb production, and mAbs to the head protein (ORF122) demonstrated specificity to ICP1 by both ELISA and a phage neutralization assay. The mAb to the head protein (ORF122) was able to detect ICP1 at biologically meaningful concentrations by Western blot analysis when ICP1 was

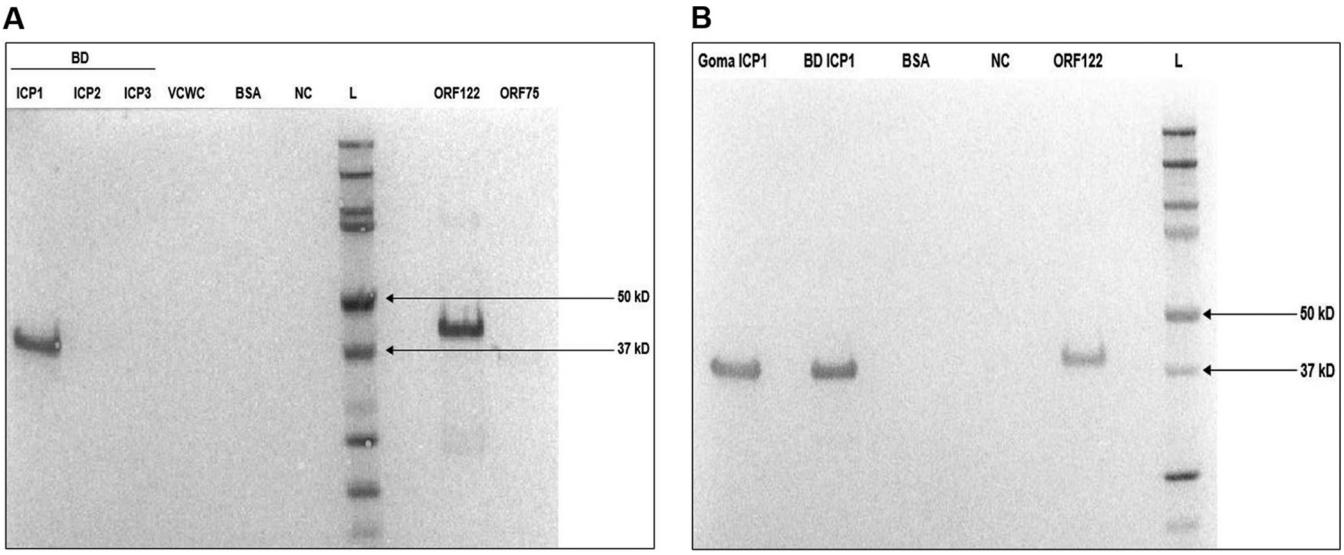


**FIG 4** Western blot analysis of candidate ICP1ORF122_mAbCL6 against ICP1 from Bangladesh (A) and Goma, DRC (B). Negative controls are ICP2 and ICP3. BD = Bangladesh, VCWC = formalin-killed *V. cholerae* whole-cell, bovine serum albumin = BSA, NC = negative control (only PBS), L = ladder (protein marker), ORF75 and ORF122 = ICP1 recombinant proteins.

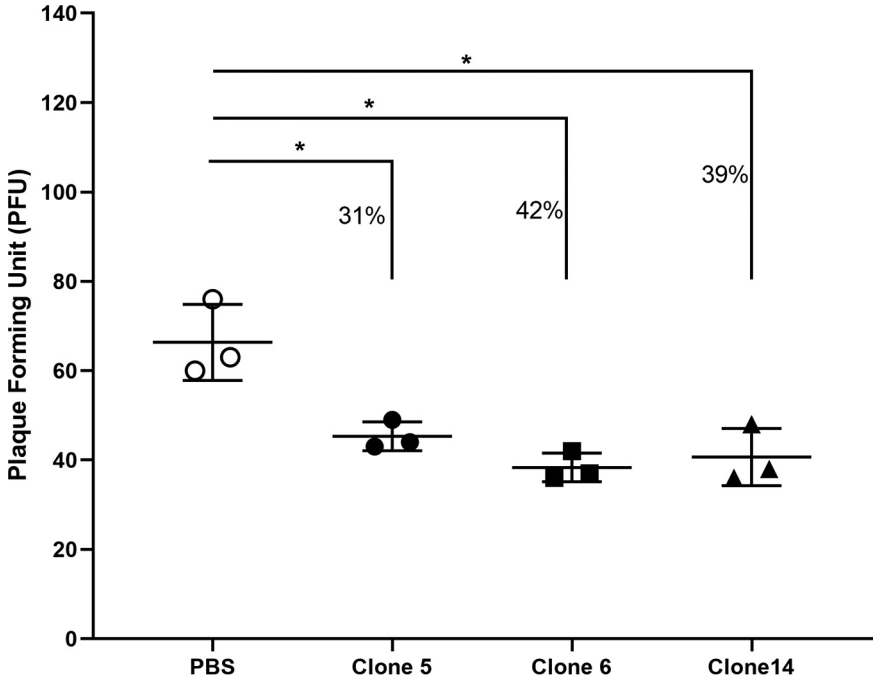


**FIG 5** ICP1 phage neutralization by ICP1ORF122_mAb CL5, CL6 and CL14. Here, PBS = phosphate-buffered saline, ICP1ORF122_mAb CL5, CL6 and CL14 represent culture supernatants from ORF122 hybridoma clones 5, 6 and 14, respectively. An asterisk denotes the statistically significant difference ($P < 0.05$) in plaque counts when ORF122 mAb mediated neutralization responses are compared with the control (PBS). Each symbol represents the average of three technical replicates for one mAb from one experiment.

spiked into cholera stool matrix. This mAb will be incorporated into an RDT prototype for evaluation in a clinical study to test our guiding hypothesis.

This approach is innovative in that we sought to develop a mAb to a pathogen-specific phage as a proxy for the bacterial pathogen. However, the durability of the approach is vulnerable if the antigenicity of the epitope varies across time and place. The strong selective pressures between bacterial 'prey' and bacteriophage 'predator' drive elaborate mech-

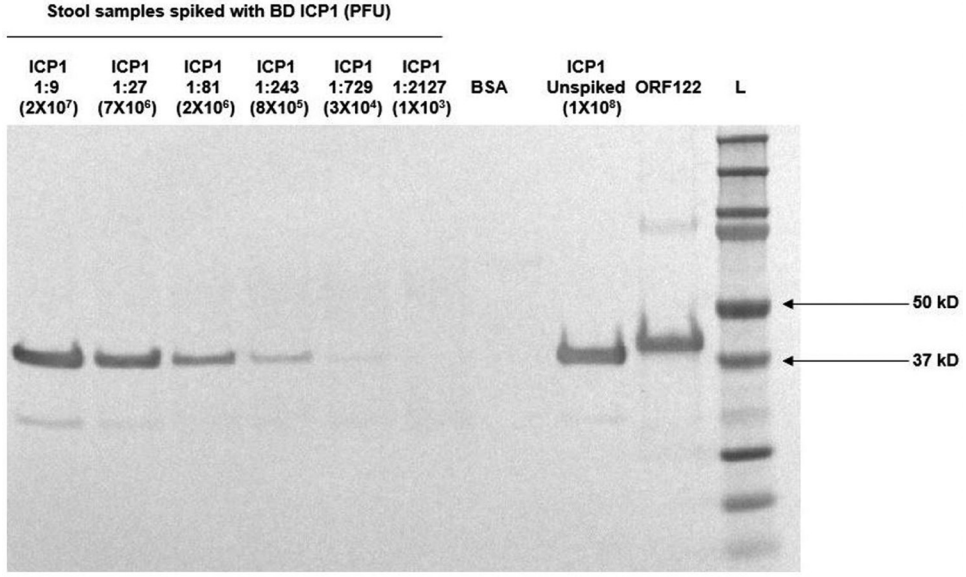


**FIG 6** Determination of the limit of detection (LOD) of ICP1ORF122_mAbCL6 against ICP1 in cholera stool supernatant. ICP1 was serially diluted in cholera stool known to be vibriophage negative (ICP1, ICP2, and ICP3 negative) in 3-fold dilution series. The concentration of the neat ICP1 stock was $2 \times 10^{10}$ PFU/mL. The lane with 1:243 dilution represents $8 \times 10^5$ PFU of ICP1 phage. Here, bovine serum albumin = BSA, ORF122 = ICP1 recombinant protein and L = ladder (protein marker).

anisms of phage immunity and escape, and, ultimately, genetic diversity. That said, genes for the candidate ICP1 structural proteins were found to be conserved. In prior analyses, the baseplate protein (ORF75) was conserved at near 100% similarity and the head protein (ORF122) was conserved at more than 99% similarity at both amino acid and nucleic acid levels (17). With additional data, we found the baseplate gene for ORF75 was more divergent compared to ORF 122 across time and location. Both proteins are unlikely to be present in non-cholera patients given that the ORFs were not detected by PCR in non-cholera patient diarrheal stool, and cross-reactivity between phages is unlikely given that no significance sequence homology beyond ICP1 was identified, including within *Myoviridae*.

The other vulnerability of our approach is that the mAb might have cross-reactivity or degrade in cholera stool matrix which harbors proteases (33, 34). Monoclonal antibodies were raised to recombinant ORF75 and ORF122 proteins, however the mAb to the baseplate protein (ORF75) failed to bind native ICP1 by ELISA, Western blot, and phage neutralization assays. This failure might be due to the lesser abundance of the epitope in the native ICP1 phage particle, post-transcriptional modification, or possibly epitope masking. This is consistent with a previous study showing that the staphylococcal phage major capsid protein was highly immunogenic, whereas the baseplate protein was found to be non-immunogenic in mice (35). On the other hand, the supernatants of the clones raised with the capsid protein ORF122 were reactive to the native ICP1 phage particle by ELISA, Western blot, and phage neutralization assays. Variability in the ELISA results between supernatants of the clones may be due to mAbs binding different epitopes; several clone supernatants saturated the assay with an absorbance of four or greater. With respect to RDT development, the candidate mAbs were able to detect ICP1 alone, without cross-reactivity to ICP2 or ICP3. During Western blot analysis, the cholera stool matrix with a ICP1 spike-in did not detectably interfere with ICP1 detection by the candidate mAbs.

These findings should be viewed within the context of the study limitations. First, the mAb did not fully ablate ICP1 in the viral neutralization assay. The mAb to ORF122 reduced plaque formation by 30 to 40% ICP1 which was less than expected, given its specificity. While this modest result is consistent with a similar study on anti-T4 head antibodies neutralizing T4 phage activity in *E. coli* (36), further optimization of the assay may be needed. The modest neutralization may be the result of cross-linking at the capsular head of ICP1 phage particles, which may leave the apparatus for binding and injecting nucleic acids into the bacterial host operative (36, 37). The rapid kinetics of the lytic cycle in prokaryotic virology, under 20 min for ICP1, may set a different expectation for neutralization assays compared to eukaryotic virology where the lytic cycle is longer (18). Second, the scope of investigation of the mAb cross-reactivity was limited, and will be improved upon by prototyping the RDT and a prospective diagnostic study in cholera and non-cholera patients. Third, we tested ICP1 spiked in cholera stool matrix alone, and we did not have access to *V. cholerae* positive stool samples immediately purged from the patient, with or without ICP1 phage at native concentrations. While the limit of detection of ICP1 in the spike-in assays was lower than that anticipated in cholera stool, data are limited on the native concentrations of ICP1 across the time course of disease. Lastly, the exact epitopes that the mAbs bind remain unmapped.

Despite limitations, our work has significant implications. The mAb to the head protein (ORF122) developed herein can be used for making an enhanced RDT to detect ICP1 as a proxy for *V. cholerae*. In a prospective diagnostic study, we will evaluate the performance of the enhanced RDT across the course of cholera outbreaks, given that cholera patients are more likely to shed virulent phage at the latter outbreak periods (11, 12, 16).

## MATERIALS AND METHODS

**Clinical sample collection.** The sample collections analyzed were from previously published Institutional Review Board (IRB) approved studies; the recruitment, consent, enrollment, and procedures are described (16, 19, 38, 39). In the first collection, stool samples from the Bangladesh study were obtained September to December 2015 at a district hospital and a subdistrict hospital in the remote northern district of Netrokona (38). In the second library, stool samples from the South Sudan study were obtained August to September 2015 at a cholera treatment center in Juba (39). The samples were collected prior to hospital administration of antibiotics; patient histories were negative for known antibiotic exposure. Lastly, microbiologic reagents were also obtained from a study in the Democratic Republic of Congo (19).

**Microbiologic procedures. (i) Bacterial strains, Phage, Media, and Growth Conditions**. We used the *V. cholerae* O1 strain HC1037 to isolate and prepare virulent phages ICP1, ICP2, and ICP3. This strain naturally lacks K139 prophage and is sensitive to ICP1, ICP2, and ICP3. The bacterial strain was grown at 37°C in Luria-Bertani (LB) broth with aeration or on LB agar plates (10, 14). The bacterial strain and phages used in this study are listed in Table S1.

**(ii) Phage preparation, isolation, and plaque assays.** We used a polyethylene glycol (PEG) precipitation method to make high titer phage stocks (15). *V. cholerae* was streaked on LB plates and incubated overnight at 37°C. A single colony from the plate was grown in LB broth to mid-exponential phase ($OD_{600}$ = 0.3). Phages were added to the culture at a multiplicity of infection (MOI) = 0.001 and incubated for 4 to 6 h. The culture suspension was spun at 10,000 × *g* for 15 min at 4°C. After 0.2 $\mu$m filter sterilization of the supernatant, 0.25 volume PEG solution (20% PEG-8000; 2.5M NaCl) was added to the supernatant and incubated at 4°C overnight for phage precipitation. Phages were pelleted by centrifugation at 10,000 × *g* for 25 min at 4°C. Phages were then washed with another round of PEG precipitation, and finally resuspended in Phage80 buffer (0.085M NaCl, 0.1 mM $MgSO_4$, 0.1 M Tris-HCl-pH 7.4). The titer of the phages was determined by plaque assay (10, 40). Phage preparation was serially diluted and incubated with mid-exponential *V. cholerae* culture for 10 min at room temperature (RT). The mixture was added to soft LB agar (0.35% Agar) media and incubated at 37°C for 3 to 4 h until plaques were observed. The number of plaques were then calculated as PFU/mL.

**Molecular procedures. (i) Cloning, expression, and purification of recombinant target proteins.** The putative baseplate protein (ORF75) and head protein (ORF122) of ICP1 phage were selected to clone and express in *Escherichia coli* (41–43); note that antigenicity of GP122 has been previously demonstrated by polyclonal antibody development by Barth et al. (44). The ORFs were amplified by PCR from genomic DNA. The primers were designed to include NdeI and XhoI restriction enzyme cutting sites at both ends of the amplified sequences. The PCR products and pET16b vector (Novagen) were digested with NdeI and XhoI at 37°C for 2 h. The target sequences were cloned into pET16b by ligation using Quick Ligation Kit (NEB). After ligation, the recombinant plasmids were transformed into DH5 *E. coli* (Novagen) to make high copy plasmids. The cloned insert sequences were verified by colony PCR and DNA sequencing. The recombinant pET16b was then transformed into *E. coli* BL21 (Novagen) to express recombinant proteins as N-terminally His-tagged fusion proteins. A single transformed colony was picked to grow overnight at 37°C in LB broth containing 100 $\mu$g/mL ampicillin. The culture was diluted to $OD_{600}$ 0.1–0.2 and incubated at 37°C in LB broth for 2 to 3 h until the $OD_{600}$ was 0.5. Expression of recombinant proteins was induced for 4 to 6 h at 37°C by adding Isopropyl $\beta$-d-1-thiogalactopyranoside to the culture at a concentration of 0.1 mM. The culture was centrifuged at 5,000 × *g* for 15 min. Before purification, an aliquot of pellet suspension and supernatant were analyzed by sodium dodecyl sulfate−polyacrylamide gel electrophoresis (SDS-PAGE) to confirm the expression of desired proteins.

The recombinant proteins were purified using His·Bind purification kit (Novagen) following manufacturer's instructions. In brief, the pellet was resuspended in Bugbuster reagent (5 mL/gm of pellet) supplemented with Benzonase Nuclease (1 $\mu$L/mL), lysozyme (1KU/mL) and protease inhibitor (10 $\mu$L/mL). The cell suspension was incubated on a shaking platform at a slow setting for 20 min at RT. After spinning at 16,000 × *g* for 20 min at 4°C, the supernatant was collected for analysis by SDS-PAGE. The pellet was resuspended and incubated again with same volume of Bugbuster reagent with lysozyme (1KU/mL) for 5 min at (RT). After the addition of equal volume of 1:10 diluted Bugbuster reagent supplemented with protease inhibitor, the suspension was spun at 5,000 × *g* for 5 min. The pellet was washed with 1:10 diluted Bugbuster reagent and centrifuged at 16,000 × *g* for 15 min at 4°C. Proteins expressed as inclusion bodies were solubilized in 8 M urea. The lysate was mixed gently with 50% Ni-NTA His-bind slurry (EMD Millipore) at 4:1 ratio on a shaking platform for 60 min at RT. The lysate-resin mixture was carefully loaded into an empty column and washed 4 times with 8 M urea (pH-6.3). Monomeric recombinant proteins were eluted with 8 M urea (pH-5.9) and multimeric proteins were eluted with 8 M urea (pH-4.5). The purity of the proteins was further assessed by SDS-PAGE analysis and the protein concentration was measured using the Bradford method.

**Immunization and antibody production in cell culture.** The purified recombinant ICP1 bacteriophage proteins were used to raise mAbs via a commercial vendor (ProMab Biotechnologies, Inc.) using a conventional hybridoma technique (28). Supernatants from 20 hybridoma clones for each of the 2 recombinant proteins from were received from the vendor.

**Immunologic assays of monoclonal antibody candidates. (i) ELISA**. ELISA was used to screen the reactivity of ORF75 and ORF122 specific-hybridoma clones to ICP1, ICP2, and ICP3 phages (45, 46). Nunc MaxiSorp plates were coated overnight at RT with ICP1 ($10^3$ PFU/well), ICP2 ($10^3$ PFU/well), ICP3 ($10^3$ PFU/well), formalin-killed *V. cholerae* (VC;$10^3$ CFU/well), ORF75 (200 ng/well), ORF122 (200 ng/well), and Bovine serum albumin (BSA; 200 ng/well). BSA and VC were used as negative controls and recombinant ORF122 or ORF75 proteins were used as positive controls. After blocking with 1% BSA-PBS, the supernatants of ORF75 and ORF122 hybridoma clones were added to the wells at 1:20 and 1:100 dilution, respectively, and incubated for 1 h at 37°C. Horseradish peroxidase-tagged goat anti-mouse IgG (Jackson ImmunoResearch) was added at 1:1000 dilution to detect antigen bound IgG mAbs. We used chromogenic substrate, 1-Step Ultra TMB to develop color. After stopping the reaction with 2 N $H_2SO_4$, the absorbance was measured at 450 nm using ELISA plate reader (max = 4). The absorbance corresponds to the antibody binding to the coated antigens.

**(ii) Western blot analysis.** The antigens were boiled with NuPAGE SDS sample buffer containing beta-mercaptoethanol for 10 min. The wells of NuPAGE 4 to 12% Bis-Tris precast gel (ThermoFisher) were loaded with ICP1 ($10^8$ PFU/well), ICP2 ($10^8$ PFU/well), ICP3 ($10^8$ PFU/well), VC ($5 \times 10^5$ CFU/well), ORF122 (2 $\mu$g/well), ORF75 (2 $\mu$g/well), and BSA (2 $\mu$g/well). To determine the limit of detection (LOD), we spiked ICP1 in VC positive and ICP1 negative stool sample and prepared a 3-fold dilution series starting from $10^8$ PFU/well. After electrophoresis at 150 V for around 40 to 50 min, the proteins from unstained gels were transferred to a nitrocellulose blotting membrane using Trans-Blot turbo Transfer System (Bio-Rad). The membrane was

blocked with 5% skim milk in Tris buffered saline (TBS) overnight at 4°C. To prepare a primary antibody, the supernatants of hybridoma clones were diluted in 5% skim milk-TBS-Tw (0.1%) at 1:500 dilution. The primary antibody was added on the membrane and incubated for 1 h with gentle shaking at RT. Following washing three times with TBS-Tw (0.1%), the membrane was incubated for 1 h with the secondary antibody, alkaline phosphatase conjugated goat anti-mouse IgG (1:5000 fold diluted in 5% skim milk-TBS-Tw) with gentle shaking at RT. The membrane was then washed three times with TBS-Tw (0.1%) and developed with 5-bromo-4-chloro-3-indolyl-phosphate/nitro blue tetrazolium (BCIP/NBT) substrate for about 5 min. The image of protein bands was captured in a gel imager (Geldoc; Bio-Rad).

**(iii) Phage neutralization assays.** Phage neutralization assays were developed and used to test neutralization/binding by each mAb to ICP1 in a biological context (47, 48). The mAbs were diluted to 20-fold in PBS and incubated with 60–100 PFU of ICP1, ICP2, and ICP3 for 1 h at 37°C. The phage-sample mixture was added to an exponential *V. cholerae* culture ($OD_{600}$ 0.3) and incubated for 7 to 10 min at RT. The mixture was then added to soft LB agar (0.35% Agar) media and incubated at 37°C for 3 to 4 h until plaques were observed. Phage neutralization was determined by comparing the plaque counts obtained from the assay without the mAb (only PBS).

**Statistical and bio-informatic analysis.** We used VaxiJen server (VaxiJen - Drug Design and Bioinformatics Lab) and IEDB tool (National Institute of Allergy and Infectious Diseases) for predicting possible antigenic ORFs of ICP1 bacteriophage (49, 50). Clustal Omega (EMBL-EBI) was used for comparing the ORF75 and ORF122 sequences of ICP1 genomes collected from different geographical locations. To compare how conserved ORF75 and ORF122 were in ICP1, alignments of 29 isolates from Bangladesh and Africa (DRC) were used; analyses were at both amino acid and nucleotide levels. The data sets were used to construct a maximum likelihood (ML) phylogeny using the program IQ-TREE (51). The ML phylogeny was then used to assess temporal signal, using the program Temp-Est (52), in order to establish how conserved the ORF75 and ORF122 are in ICP1. The MSA alignment was then plotted using the R package ggmsa (http://yulab-smu.top/ggmsa/), and the temporal signal was plotted in R using ggplot2 and custom R scripts (53).

GraphPad Prism version 8 (GraphPad Software, Inc.) was used for statistical analyses and graphical presentation. The differences in antigen specific antibody responses were statistically evaluated by paired *t* test. We also used the paired *t* test to compare the antibody mediated phage neutralization with control. The differences were considered as statistically significant if *P* value was less than 0.05.

**Data availability.** Data analyzed are presented within the paper and supplemental material.

## SUPPLEMENTAL MATERIAL

Supplemental material is available online only.

**SUPPLEMENTAL FILE 1**, PDF file, 0.4 MB.

## ACKNOWLEDGMENTS

We thank the patients for participating in the studies from which the clinical samples were obtained. We are grateful to Randy Autrey and Krista Berquist for their administrative expertise, as well as the UF Emerging Pathogens Institute and the UF Department of Pediatrics for providing vital infrastructure.

This work was supported by a grant from the Wellcome Trust to E.J.N. (DFID grant 215676/Z) and internal support from the Emerging Pathogens Institute, the Department of Pediatrics and the Department of Environmental and Global Health at the University of Florida, and a grant from the NIH (USA) to A.C. (AI055058).

The funders had no role in the study design, data collection and analysis, decision to publish, or preparation of the manuscript.

We report no conflicts of interest.

## REFERENCES

1. Anonymous. 2017. Cholera, 2016. Wkly Epidemiol Rec 92:521–530. https://apps.who.int/iris/bitstream/handle/10665/258911/WER9236-521-530.pdf.
2. Azman AS, Moore SM, Lessler J. 2020. Surveillance and the global fight against cholera: setting priorities and tracking progress. Vaccine 38:A28–A30. https://doi.org/10.1016/j.vaccine.2019.06.037.
3. Emch M, Feldacker C, Islam MS, Ali M. 2008. Seasonality of cholera from 1974 to 2005: a review of global patterns. Int J Health Geogr 7:31. https://doi.org/10.1186/1476-072X-7-31.
4. Ganesan D, Gupta SS, Legros D. 2020. Cholera surveillance and estimation of burden of cholera. Vaccine 38:A13–A17. https://doi.org/10.1016/j.vaccine.2019.07.036.
5. Ali M, Nelson AR, Lopez AL, Sack DA. 2015. Updated global burden of cholera in endemic countries. PLoS Negl Trop Dis 9:e0003832. https://doi.org/10.1371/journal.pntd.0003832.
6. Cash RA, Narasimhan V. 2000. Impediments to global surveillance of infectious diseases: consequences of open reporting in a global economy. Bull World Health Organ 78:1358–1367. https://www.ncbi.nlm.nih.gov/pmc/articles/PMC2560626/pdf/11143197.pdf.
7. Zumla A, Hui DSC. 2019. Emerging and reemerging infectious diseases: global overview. Infect Dis Clin North Am 33:xiii–xxix. https://doi.org/10.1016/j.idc.2019.09.001.
8. Clemens JD, Nair GB, Ahmed T, Qadri F, Holmgren J. 2017. Cholera. Lancet 390:1539–1549. https://doi.org/10.1016/S0140-6736(17)30559-7.
9. Harris JB, LaRocque RC, Qadri F, Ryan ET, Calderwood SB. 2012. Cholera. Lancet 379:2466–2476. https://doi.org/10.1016/S0140-6736(12)60436-X.
10. Nelson EJ, Chowdhury A, Flynn J, Schild S, Bourassa L, Shao Y, LaRocque RC, Calderwood SB, Qadri F, Camilli A. 2008. Transmission of *Vibrio cholerae* is antagonized by lytic phage and entry into the aquatic environment. PLoS Pathog 4:e1000187. https://doi.org/10.1371/journal.ppat.1000187.
11. Faruque SM, Islam MJ, Ahmad QS, Faruque AS, Sack DA, Nair GB, Mekalanos JJ. 2005. Self-limiting nature of seasonal cholera epidemics: role of host-

mediated amplification of phage. Proc Natl Acad Sci U S A 102:6119–6124. https://doi.org/10.1073/pnas.0502069102.
12. Faruque SM, Naser IB, Islam MJ, Faruque AS, Ghosh AN, Nair GB, Sack DA, Mekalanos JJ. 2005. Seasonal epidemics of cholera inversely correlate with the prevalence of environmental cholera phages. Proc Natl Acad Sci U S A 102:1702–1707. https://doi.org/10.1073/pnas.0408992102.
13. Faruque SM. 2014. Role of phages in the epidemiology of cholera. Curr Top Microbiol Immunol 379:165–180. https://doi.org/10.1007/82_2013_358.
14. Seed KD, Bodi KL, Kropinski AM, Ackermann HW, Calderwood SB, Qadri F, Camilli A. 2011. Evidence of a dominant lineage of *Vibrio cholerae*-specific lytic bacteriophages shed by cholera patients over a 10-year period in Dhaka, Bangladesh. mBio 2:e00334-10. https://doi.org/10.1128/mBio.00334-10.
15. Yen M, Cairns LS, Camilli A. 2017. A cocktail of three virulent bacteriophages prevents *Vibrio cholerae* infection in animal models. Nat Commun 8:14187. https://doi.org/10.1038/ncomms14187.
16. Nelson EJ, Grembi JA, Chao DL, Andrews JR, Alexandrova L, Rodriguez PH, Ramachandran VV, Sayeed MA, Wamala JF, Debes AK, Sack DA, Hryckowian AJ, Haque F, Khatun S, Rahman M, Chien A, Spormann AM, Schoolnik GK. 2020. Gold standard cholera diagnostics are tarnished by lytic bacteriophage and antibiotics. J Clin Microbiol 58:e00412-20. https://doi.org/10.1128/JCM.00412-20.
17. Angermeyer A, Das MM, Singh DV, Seed KD. 2018. Analysis of 19 highly conserved *Vibrio cholerae* bacteriophages isolated from environmental and patient sources over a twelve-year period. Viruses 10:299. https://doi.org/10.3390/v10060299.
18. Boyd CM, Angermeyer A, Hays SG, Barth ZK, Patel KM, Seed KD. 2021. Bacteriophage ICP1: a persistent predator of *Vibrio cholerae*. Annu Rev Virol 8:285–304. https://doi.org/10.1146/annurev-virology-091919-072020.
19. Alam MT, Mavian C, Salemi M, Tagliamonte MS, Paisie T, Cash MN, Angermeyer A, Seed KD, Camilli A, Maisha FM, Senga RKK, Morris JG, Ali A. 2021. *Vibrio cholerae* multifaceted adaptive strategies in response to bacteriophage predation in an endemic region of the Democratic Republic of the Congo. medRxiv. https://doi.org/10.1101/2021.07.30.21261389.
20. Gobal Task Force on Cholera Control (GTFCC) Surveillance Working Group, WHO. 2017. Interim Guidance Document on Cholera Surveillance. https://www.gtfcc.org/wp-content/uploads/2019/10/gtfcc-interim-guidance-document-on-cholera-surveillance.pdf.
21. Tukei PM. 1996. Emerging and re-emerging infectious diseases: a global health threat. Afr J Health Sci 3:27. https://europepmc.org/article/med/17451292.
22. Chibwe I, Kasambara W, Kagoli M, Milala H, Gondwe C, Azman AS. 2020. Field evaluation of cholkit rapid diagnostic test for *Vibrio Cholerae* O1 during a cholera outbreak in Malawi, 2018. Open Forum Infect Dis 7. https://doi.org/10.1093/ofid/ofaa493.
23. Page AL, Alberti KP, Mondonge V, Rauzier J, Quilici ML, Guerin PJ. 2012. Evaluation of a rapid test for the diagnosis of cholera in the absence of a gold standard. PLoS One 7:e37360. https://doi.org/10.1371/journal.pone.0037360.
24. Dick MH, Guillerm M, Moussy F, Chaignat CL. 2012. Review of two decades of cholera diagnostics–how far have we really come? PLoS Negl Trop Dis 6:e1845. https://doi.org/10.1371/journal.pntd.0001845.
25. Sinha A, Sengupta S, Ghosh S, Basu S, Sur D, Kanungo S, Mukhopadhyay AK, Ramamurthy T, Nagamani K, Rao MN, Nandy RK. 2012. Evaluation of a rapid dipstick test for identifying cholera cases during the outbreak. Indian J Med Res 135:523–528.
26. Debes AK, Ateudjieu J, Guenou E, Ebile W, Sonkoua IT, Njimbia AC, Steinwald P, Ram M, Sack DA. 2016. Clinical and environmental surveillance for *Vibrio cholerae* in resource constrained areas: application during a 1-year surveillance in the far north region of Cameroon. Am J Trop Med Hyg 94:537–543. https://doi.org/10.4269/ajtmh.15-0496.
27. Alam M, Hasan NA, Sultana M, Nair GB, Sadique A, Faruque AS, Endtz HP, Sack RB, Huq A, Colwell RR, Izumiya H, Morita M, Watanabe H, Cravioto A. 2010. Diagnostic limitations to accurate diagnosis of cholera. J Clin Microbiol 48:3918–3922. https://doi.org/10.1128/JCM.00616-10.
28. Sayeed MA, Islam K, Hossain M, Akter NJ, Alam MN, Sultana N, Khanam F, Kelly M, Charles RC, Kováč P, Xu P, Andrews JR, Calderwood SB, Amin J, Ryan ET, Qadri F. 2018. Development of a new dipstick (Cholkit) for rapid detection of *Vibrio cholerae* O1 in acute watery diarrheal stools. PLoS Negl Trop Dis 12:e0006286. https://doi.org/10.1371/journal.pntd.0006286.
29. Benenson AS, Islam MR, Greenough WB, 3rd. 1964. Rapid identification of *Vibrio Cholerae* by darkfield microscopy. Bull World Health Organ 30:827–831.
30. Bhuiyan NA, Qadri F, Faruque AS, Malek MA, Salam MA, Nato F, Fournier JM, Chanteau S, Sack DA, Balakrish Nair G. 2003. Use of dipsticks for rapid diagnosis of cholera caused by *Vibrio cholerae* O1 and O139 from rectal swabs. J Clin Microbiol 41:3939–3941. https://doi.org/10.1128/JCM.41.8.3939-3941.2003.
31. Nato F, Boutonnier A, Rajerison M, Grosjean P, Dartevelle S, Guénolé A, Bhuiyan NA, Sack DA, Nair GB, Fournier JM, Chanteau S. 2003. One-step immunochromatographic dipstick tests for rapid detection of *Vibrio cholerae* O1 and O139 in stool samples. Clin Diagn Lab Immunol 10:476–478. https://doi.org/10.1128/cdli.10.3.476-478.2003.
32. Qadri F, Hasan JA, Hossain J, Chowdhury A, Begum YA, Azim T, Loomis L, Sack RB, Albert MJ. 1995. Evaluation of the monoclonal antibody-based kit Bengal SMART for rapid detection of *Vibrio cholerae* O139 synonym Bengal in stool samples. J Clin Microbiol 33:732–734. https://doi.org/10.1128/jcm.33.3.732-734.1995.
33. Carroll IM, Ringel-Kulka T, Ferrier L, Wu MC, Siddle JP, Bueno L, Ringel Y. 2013. Fecal protease activity is associated with compositional alterations in the intestinal microbiota. PLoS One 8:e78017. https://doi.org/10.1371/journal.pone.0078017.
34. Funabashi R, Miyakawa K, Yamaoka Y, Yoshimura S, Yamane S, Jeremiah SS, Shimizu K, Ozawa H, Kawakami C, Usuku S, Tanaka N, Yamazaki E, Kimura H, Hasegawa H, Ryo A. 2021. Development of highly sensitive and rapid antigen detection assay for diagnosis of COVID-19 utilizing optical waveguide immunosensor. J Mol Cell Biol 13:763–766. https://doi.org/10.1093/jmcb/mjab037.
35. Majewska J, Kaźmierczak Z, Lahutta K, Lecion D, Szymczak A, Miernikiewicz P, Drapała J, Harhala M, Marek-Bukowiec K, Jędruchniewicz N, Owczarek B, Górski A, Dąbrowska K. 2019. Induction of phage-specific antibodies by two therapeutic Staphylococcal bacteriophages administered per os. Front Immunol 10:2607. https://doi.org/10.3389/fimmu.2019.02607.
36. Dąbrowska K, Miernikiewicz P, Piotrowicz A, Hodyra K, Owczarek B, Lecion D, Kaźmierczak Z, Letarov A, Górski A. 2014. Immunogenicity studies of proteins forming the T4 phage head surface. J Virol 88:12551–12557. https://doi.org/10.1128/JVI.02043-14.
37. Jerne NK, Avegno P. 1956. The development of the phage-inactivating properties of serum during the course of specific immunization of an animal: reversible and irreversible inactivation. J Immunol 76:200–208.
38. Haque F, Ball RL, Khatun S, Ahmed M, Kache S, Chisti MJ, Sarker SA, Maples SD, Pieri D, Vardhan Korrapati T, Sarnquist C, Federspiel N, Rahman MW, Andrews JR, Rahman M, Nelson EJ. 2017. Evaluation of a smartphone decision-support tool for diarrheal disease management in a resource-limited setting. PLoS Negl Trop Dis 11:e0005290. https://doi.org/10.1371/journal.pntd.0005290.
39. Ontweka LN, Deng LO, Rauzier J, Debes AK, Tadesse F, Parker LA, Wamala JF, Bior BK, Lasuba M, But AB, Grandesso F, Jamet C, Cohuet S, Ciglenecki I, Serafini M, Sack DA, Quilici ML, Azman AS, Luquero FJ, Page AL. 2016. Cholera rapid test with enrichment step has diagnostic performance equivalent to culture. PLoS One 11:e0168257. https://doi.org/10.1371/journal.pone.0168257.
40. Nelson EJ, Chowdhury A, Harris JB, Begum YA, Chowdhury F, Khan AI, Larocque RC, Bishop AL, Ryan ET, Camilli A, Qadri F, Calderwood SB. 2007. Complexity of rice-water stool from patients with *Vibrio cholerae* plays a role in the transmission of infectious diarrhea. Proc Natl Acad Sci U S A 104:19091–19096. https://doi.org/10.1073/pnas.0706352104.
41. Hu YF, Zhao D, Yu XL, Hu YL, Li RC, Ge M, Xu TQ, Liu XB, Liao HY. 2017. Identification of bacterial surface antigens by screening peptide phage libraries using whole bacteria cell-purified antisera. Front Microbiol 8:82. https://doi.org/10.3389/fmicb.2017.00082.
42. Mora M, Bensi G, Capo S, Falugi F, Zingaretti C, Manetti AG, Maggi T, Taddei AR, Grandi G, Telford JL. 2005. Group A *Streptococcus* produce pilus-like structures containing protective antigens and Lancefield T antigens. Proc Natl Acad Sci U S A 102:15641–15646. https://doi.org/10.1073/pnas.0507808102.
43. Gupta A, Grove A. 2014. Ligand-binding pocket bridges DNA-binding and dimerization domains of the urate-responsive MarR homologue MftR from *Burkholderia thailandensis*. Biochemistry 53:4368–4380. https://doi.org/10.1021/bi500219t.
44. Barth ZK, Netter Z, Angermeyer A, Bhardwaj P, Seed KD. 2020. A Family of viral satellites manipulates invading virus gene expression and can affect cholera toxin mobilization. mSystems 5:e00358-20. https://doi.org/10.1128/mSystems.00358-20.
45. Sayeed MA, Bufano MK, Xu P, Eckhoff G, Charles RC, Alam MM, Sultana T, Rashu MR, Berger A, Gonzalez-Escobedo G, Mandlik A, Bhuiyan TR, Leung DT, LaRocque RC, Harris JB, Calderwood SB, Qadri F, Vann WF, Kovac P, Ryan ET. 2015. A cholera conjugate vaccine containing O-specific Polysaccharide (OSP) of *V. cholerae* O1 Inaba and recombinant fragment of

tetanus toxin heavy chain (OSP:rTTHc) induces serum, memory and lamina proprial responses against OSP and is protective in mice. PLoS Negl Trop Dis 9:e0003881. https://doi.org/10.1371/journal.pntd.0003881.
46. Kauffman RC, Bhuiyan TR, Nakajima R, Mayo-Smith LM, Rashu R, Hoq MR, Chowdhury F, Khan AI, Rahman A, Bhaumik SK, Harris L, O'Neal JT, Trost JF, Alam NH, Jasinskas A, Dotsey E, Kelly M, Charles RC, Xu P, Kovac P, Calderwood SB, Ryan ET, Felgner PL, Qadri F, Wrammert J, Harris JB. 2016. Single-cell analysis of the plasmablast response to *Vibrio cholerae* demonstrates expansion of cross-reactive memory B cells. mBio 7:e02021-16. https://doi.org/10.1128/mBio.02021-16.
47. Priyamvada L, Quicke KM, Hudson WH, Onlamoon N, Sewatanon J, Edupuganti S, Pattanapanyasat K, Chokephaibulkit K, Mulligan MJ, Wilson PC, Ahmed R, Suthar MS, Wrammert J. 2016. Human antibody responses after dengue virus infection are highly cross-reactive to Zika virus. Proc Natl Acad Sci U S A 113:7852–7857. https://doi.org/10.1073/pnas.1607931113.
48. Priyamvada L, Cho A, Onlamoon N, Zheng NY, Huang M, Kovalenkov Y, Chokephaibulkit K, Angkasekwinai N, Pattanapanyasat K, Ahmed R, Wilson PC, Wrammert J. 2016. B cell responses during secondary dengue virus infection are dominated by highly cross-reactive, memory-derived plasmablasts. J Virol 90:5574–5585. https://doi.org/10.1128/JVI.03203-15.
49. Doytchinova IA, Flower DR. 2007. VaxiJen: a server for prediction of protective antigens, tumour antigens and subunit vaccines. BMC Bioinformatics 8:4. https://doi.org/10.1186/1471-2105-8-4.
50. Larsen JE, Lund O, Nielsen M. 2006. Improved method for predicting linear B-cell epitopes. Immunome Res 2:2. https://doi.org/10.1186/1745-7580-2-2.
51. Nguyen LT, Schmidt HA, von Haeseler A, Minh BQ. 2015. IQ-TREE: a fast and effective stochastic algorithm for estimating maximum-likelihood phylogenies. Mol Biol Evol 32:268–274. https://doi.org/10.1093/molbev/msu300.
52. Rambaut A, Lam TT, Max Carvalho L, Pybus OG. 2016. Exploring the temporal structure of heterochronous sequences using TempEst (formerly Path-O-Gen). Virus Evol 2. https://doi.org/10.1093/ve/vew007.
53. Villanueva RAM, Chen ZJ. 2019. ggplot2: Elegant Graphics for Data Analysis (2nd ed). Measure: Interdisc Res and Persp17:160–167. https://doi.org/10.1080/15366367.2019.1565254.